FUDMA Journal of Sciences (FJS)
ISSN online: 2616-1370
ISSN print: 2645 - 2944
Vol. 10 No. 7, April, 2026, pp 329 – 337
DOI: https://doi.org/10.33003/fjs-2026-1007-5261

SATELLITE-BASED ESTIMATION AND TREND ANALYSIS OF $PM_{2.5}$ CONCENTRATION USING MODIS MAIAC AEROSOL OPTICAL DEPTH OVER THE UNIVERSITY OF BENIN, NIGERIA

***[1]Stephen Olushola Oladosu, [1]Tolulope Samuel Fawale, [1]Kelvin Akere Moses, [2]Rachael Omoniyepe Oladosu, [1]Godsent Efosa Felix, [1]Enobore Kelly Igbinidu and [1]Mabel Eghemenrior Alenkhe**

[1]Department of Geomatics, Faculty of Environmental Sciences, University of Benin, Benin City, Nigeria;
[2]Department of Health Promotion and Environmental Health Education, Faculty of Education, University of Ilorin, Ilorin, Nigeria.

*Corresponding authors' email: olushola.oladosu@uniben.edu Phone: +2348065211810

ABSTRACT

Atmospheric aerosol pollution remains a major environmental and public health concern in rapidly urbanizing regions with limited air-quality monitoring infrastructure. This study developed a satellite-based framework for estimating and analyzing $PM_{2.5}$ concentration over the University of Benin, Nigeria, using MODIS MAIAC Aerosol Optical Depth (AOD) data integrated with ground-based observations. High-resolution AOD data spanning 2015–2024 were processed within Google Earth Engine and calibrated using monthly $PM_{2.5}$ measurements from two monitoring locations. A linear regression model produced a moderate positive relationship between AOD and $PM_{2.5}$ ($R = 0.54$; $R^2 = 0.29$), indicating that approximately 29% of $PM_{2.5}$ variability could be explained by aerosol loading. Although the explanatory power is moderate, such behaviour is common in humid tropical environments where cloud cover, aerosol mixing, atmospheric humidity, and boundary-layer dynamics weaken the AOD–$PM_{2.5}$ relationship. Seasonal Mann–Kendall analysis revealed a statistically significant decreasing Harmattan AOD trend ($p = 0.0031$) with a Sen's slope of −0.046 AOD per season. Estimated $PM_{2.5}$ concentrations also exhibited decreasing seasonal trends ranging from approximately −0.997 to −1.20 $\mu g/m^3$ per season across calibration approaches. The study demonstrates that satellite observations, when locally calibrated, can support seasonal aerosol monitoring and long-term environmental assessment in data-scarce tropical environments. The framework further highlights the potential of low-cost satellite-based air-quality surveillance for campus-scale environmental management and exposure assessment.

Keywords: Aerosol Optical Depth, $PM_{2.5}$, MODIS MAIAC, Harmattan, Trend Analysis, Remote Sensing

INTRODUCTION

Air quality degradation due to increasing atmospheric aerosol concentrations has become a major environmental and public health concern, particularly in rapidly urbanizing regions of developing countries. Aerosols, including dust and fine particulate matter ($PM_{2.5}$), have been strongly linked to respiratory and cardiovascular diseases, reduced visibility, and broader climate impacts (Marone et al., 2020; Atuyambe *et al.*, 2024). Long-term exposure to airborne particulate matter has also been associated with accelerated lung aging and chronic respiratory complications (Eckhardt & Wu, 2021; Hu & Rao, 2009). In West Africa, these impacts are further intensified during the Harmattan season, when dry and dust-laden winds originating from the Sahara Desert significantly elevate aerosol loading across the region (Ogunjo *et al.*, 2022). University environments, such as the University of Benin, represent densely populated micro-urban systems where anthropogenic activities including vehicular emissions, construction, and energy use, contribute to localized air pollution. Despite the potential health risks to students and staff, routine monitoring of particulate matter remains limited due to the high cost and maintenance requirements of ground-based air quality instruments (Rahal, 2020; Ramírez *et al.*, 2023). This creates a critical gap in environmental data needed for effective air quality management and policy formulation (United Nations Environment Programme, {UNEP, 2021}).

Satellite remote sensing offers a viable alternative for large-scale and long-term air quality monitoring. In particular, Aerosol Optical Depth (AOD), derived from instruments such as the Moderate Resolution Imaging Spectroradiometer (MODIS), provides a quantitative measure of atmospheric aerosol loading and has been widely used as a proxy for surface-level particulate matter concentrations (Gupta & Christopher, 2009; van Donkelaar *et al.*, 2010). The MODIS MAIAC product further improves retrieval accuracy over heterogeneous land surfaces, making it suitable for urban and peri-urban environments (Lyapustin *et al.*, 2018). Several studies have demonstrated the feasibility of estimating $PM_{2.5}$ concentrations from satellite-derived AOD using statistical and machine learning approaches (Chew *et al.*, 2016; Li *et al.*, 2024; Logothetis *et al.*, 2024). Recent advances in deep learning techniques have further improved airborne particulate matter sensing and aerosol estimation capabilities (Chauhan *et al.*, 2025). However, the strength of this relationship varies significantly across regions due to meteorological conditions, aerosol composition, and vertical atmospheric structure. Consequently, locally calibrated models are essential for improving estimation accuracy, particularly in tropical environments where cloud cover and humidity introduce additional uncertainty.

Despite the increasing use of satellite remote sensing for regional and continental aerosol monitoring, limited attention has been given to campus-scale environments within rapidly urbanizing tropical cities in Nigeria. University campuses represent unique micro-urban systems characterized by concentrated human activities, vehicular movement, residential density, and localized emission sources that may significantly influence aerosol behaviour and exposure patterns. Yet, routine air-quality monitoring within many Nigerian universities remains absent due to financial and technical limitations associated with ground-based instrumentation. Consequently, there is limited understanding of long-term particulate pollution dynamics within these institutional environments, particularly during Harmattan periods when aerosol loading intensifies across West Africa.

This study therefore addresses this gap by developing a satellite-based framework for estimating $PM_{2.5}$ concentrations over the University of Benin using MODIS MAIAC AOD data integrated with ground-based observations. Specifically, the study goals are to: (i) establish a statistical relationship between AOD and $PM_{2.5}$ using locally calibrated regression models; (ii) analyze seasonal and long-term trends in aerosol loading from 2015 to 2024; and (iii) evaluate the feasibility of satellite-derived air quality monitoring for supporting environmental management in data-limited regions.

MATERIALS AND METHODS

Study Area Description

The study was conducted at the University of Benin (UNIBEN), Ugbowo Campus, located in Benin City, Edo State, Nigeria. The geographic extent of the study area, expressed in Universal Transverse Mercator (UTM Zone 31N), ranges between 788666.50 mE to 790748.71 mE and 707944.94 mN to 708442.54 mN. The campus represents a densely populated academic and residential environment with an estimated population exceeding 40,000 students and approximately 8,000 staff members. This makes it a suitable micro-urban environment for assessing localized air quality dynamics. Climatically, the study area lies within a humid tropical zone characterized by two dominant seasons: the wet season (April–October) and the dry season (November–March). The dry season is strongly influenced by the Harmattan phenomenon, during which dust-laden winds from the Sahara Desert significantly increase atmospheric aerosol concentrations across West Africa (Ogunjo *et al*., 2022). A spatial representation of the study area is presented in Figure 1, illustrating the geographic extent and environmental context of the analysis.

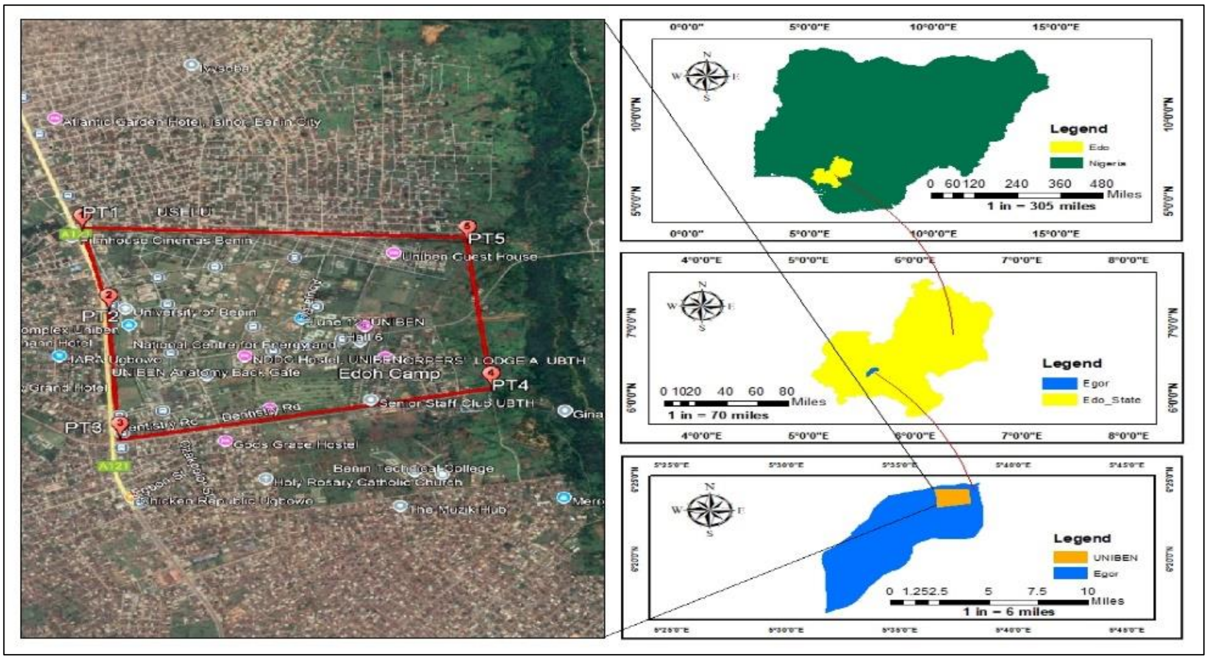

Figure 1: Study Area Map Showing University of Benin

Data Sources

This study integrates satellite-derived aerosol data with ground-based particulate matter observations to estimate $PM_{2.5}$ concentrations and analyze long-term trends.

MODIS MAIAC Aerosol Optical Depth Data

Aerosol Optical Depth (AOD) data were obtained from the MODIS MAIAC product (MCD19A2, Collection 6.1), which provides high-resolution (1 km) aerosol retrievals with improved performance over heterogeneous land surfaces (Lyapustin *et al*., 2018; Bodhaine et al, 1999). Accurate aerosol optical depth retrieval remains fundamental for atmospheric pollution assessment and environmental monitoring (Chylek et al., 2005). The AOD parameter used corresponds to a wavelength of 0.47 µm, which is particularly sensitive to fine-mode aerosols associated with anthropogenic pollution and transported dust (National Aeronautics and Space Administration {NASA, 2026}). The dataset spans a 10-year period (2015–2024) and was accessed and processed using Google Earth Engine (GEE).

Ground-Based $PM_{2.5}$ Data

Ground-based $PM_{2.5}$ measurements were obtained from two monitoring stations within Benin City: University of Benin Station (Primary Dataset): Located within the study area and used for model calibration. Palm House Station (Secondary Dataset): Located in a more urbanized environment and used for validation.

Daily observations from both stations were aggregated into monthly averages to ensure consistency with satellite-derived AOD data. The integration of both datasets enables spatial comparison and validation of the developed regression model.

Data Processing in Google Earth Engine

Satellite data processing was carried out within the Google Earth Engine platform to ensure efficient handling of large geospatial datasets (Pham-Duc et al. 2023).

AOD Scaling

Atmospheric optical depth retrievals are also influenced by Rayleigh scattering effects associated with atmospheric molecules (Bodhaine et al., 1999). MODIS MAIAC AOD values are stored as scaled integers and were converted into physically meaningful values using a scaling factor of 0.001, as shown in equation (1):

$$AOD = AOD_{raw} \times 0.001 \quad (1)$$

This scaling ensures that the retrieved values represent actual atmospheric aerosol optical depth. The workflow for AOD acquisition and scaling is illustrated in Figure 2.

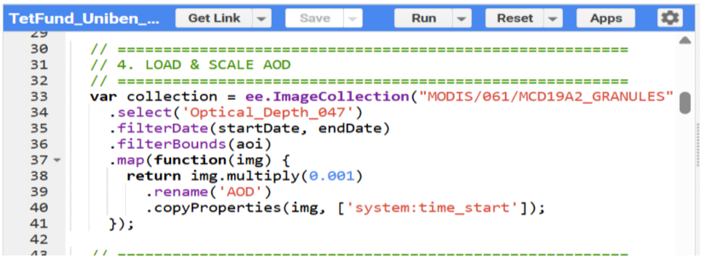

```
// =======================================================
// 4. LOAD & SCALE AOD
// =======================================================
var collection = ee.ImageCollection("MODIS/061/MCD19A2_GRANULES")
  .select('Optical_Depth_047')
  .filterDate(startDate, endDate)
  .filterBounds(aoi)
  .map(function(img) {
    return img.multiply(0.001)
      .rename('AOD')
      .copyProperties(img, ['system:time_start']);
  });
```

Figure 2: MODIS MAIAC AOD Data Acquisition and Scaling

Daily Aggregation

Due to multiple satellite overpasses within a single day, daily AOD values were computed by averaging all available observations:

$$AOD_{daily} = \frac{1}{n}\sum_{i=1}^{n} AOD_i \quad (2)$$

Where n represents the number of observations per day. The aggregation process is illustrated in Figure 3

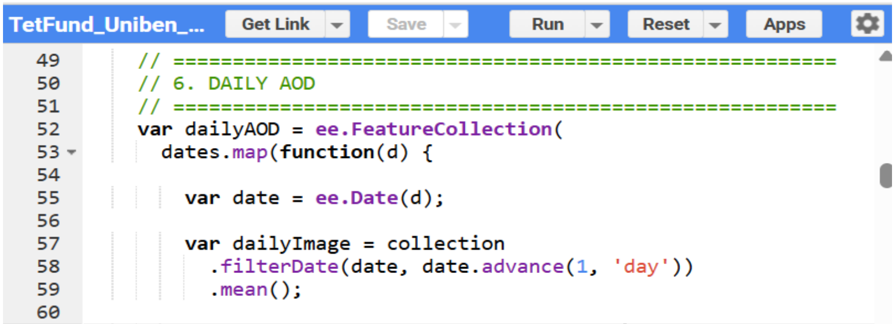

```
// =======================================================
// 6. DAILY AOD
// =======================================================
var dailyAOD = ee.FeatureCollection(
  dates.map(function(d) {

    var date = ee.Date(d);

    var dailyImage = collection
      .filterDate(date, date.advance(1, 'day'))
      .mean();

```

Figure 3: Daily AOD Aggregation

Spatial Averaging

To obtain a representative value for the study area, spatial averaging was performed across all pixels within the Area of Interest (AOI):

$$AOD_{mean} = \frac{1}{N}\sum_{j=1}^{N} AOD_j \quad (3)$$

Where N is the total number of pixels within the AOI. This approach minimizes spatial noise and enhances robustness. The process is shown in Figure 4.

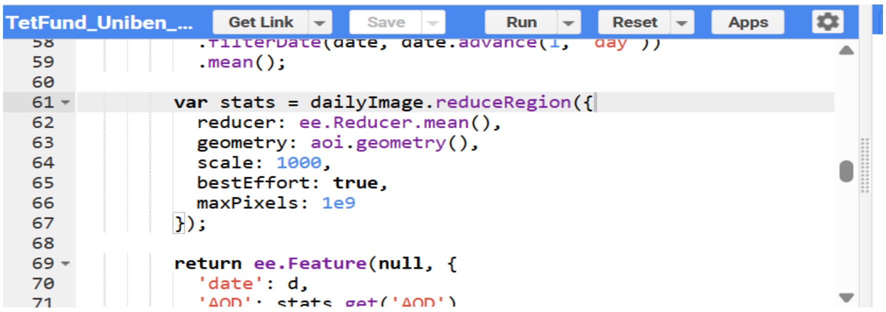

```
      .filterDate(date, date.advance(1, 'day'))
      .mean();

    var stats = dailyImage.reduceRegion({
      reducer: ee.Reducer.mean(),
      geometry: aoi.geometry(),
      scale: 1000,
      bestEffort: true,
      maxPixels: 1e9
    });

    return ee.Feature(null, {
      'date': d,
      'AOD': stats.get('AOD')
```

Figure 4: AOD Spatial Averaging

Handling Missing Data

Cloud cover and atmospheric interference often result in missing AOD values. In this study, only valid (non-null) observations were retained, while missing values were excluded. Unlike conventional approaches, strict quality assurance (QA) filtering was not applied in order to preserve temporal coverage, particularly in tropical environments where cloud contamination is frequent (Zhang *et al*., 2017).

Estimation of PM₂.₅ from Aerosol Optical Depth

The relationship between AOD and $PM_{2.5}$ was modeled using linear regression based on the framework established by (Gupta and Christopher, 2009; van Donkelaar *et al*., 2010) which demonstrated that AOD can serve as a proxy for surface particulate matter concentrations.

The linear model is expressed as:

$$PM_{2.5} = m \cdot AOD + c \quad (4)$$

Where: m is the slope (sensitivity of $PM_{2.5}$ to AOD) c is the intercept (background $PM_{2.5}$ concentration).

The derived regression model is expressed as:

$$PM_{2.5} = 25.51 \cdot AOD + 22.32$$

Ordinary Least Squares (OLS) Estimation

Model parameters were estimated using Ordinary Least Squares (OLS), which minimizes the sum of squared residuals (Montgomery *et al*., 2012):

$$S = \sum_{i=1}^{n} (y_i - (mx_i + c))^2 \quad (5)$$

By setting partial derivatives to zero, the optimal parameters are obtained using equations 6 and 7:

$$m = \frac{\sum(x_i - \bar{x})(y_i - \bar{y})}{\sum(x_i - \bar{x})^2} \quad (6)$$

$$c = \bar{y} - m\bar{x} \quad (7)$$

Where $\bar{x}$ and $\bar{y}$ represent mean values of AOD and PM₂.₅, respectively. The regression workflow is illustrated in Figure 5.

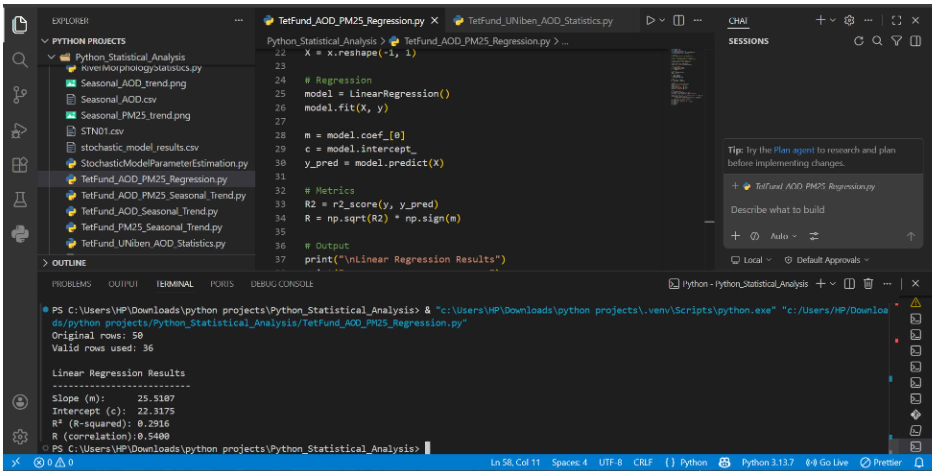

```python
X = x.reshape(-1, 1)

# Regression
model = LinearRegression()
model.fit(X, y)

m = model.coef_[0]
c = model.intercept_
y_pred = model.predict(X)

# Metrics
R2 = r2_score(y, y_pred)
R = np.sqrt(R2) * np.sign(m)

# Output
print("\nLinear Regression Results")
```

```
PS C:\Users\HP\Downloads\python projects\Python_Statistical_Analysis> & "c:\Users\HP\Downloads\python projects\.venv\Scripts\python.exe" "c:/Users/HP/Downloa
ds/python projects/Python_Statistical_Analysis/TetFund_AOD_PM25_Regression.py"
Original rows: 50
Valid rows used: 36

Linear Regression Results
-------------------------
Slope (m):       25.5107
Intercept (c):   22.3175
R² (R-squared): 0.2916
R (correlation):0.5400
PS C:\Users\HP\Downloads\python projects\Python_Statistical_Analysis>
```

Figure 5: Regression Model Workflow

Model Evaluation Metrics

The coefficient of determination (R²), as described by Draper and Smith (1998), was used to evaluate model performance:

$$R^2 = 1 - \frac{\sum(y_i - \hat{y}_i)^2}{\sum(y_i - \bar{y})^2} \quad (8)$$

The correlation coefficient (R) was computed as with the aid of equation 9:

$$R = \sqrt{R^2} \quad (9)$$

These metrics quantify the strength and direction of the relationship between AOD and PM₂.₅. Using the observed dataset, the regression coefficients were obtained as stated ealier under the application of equation 4.

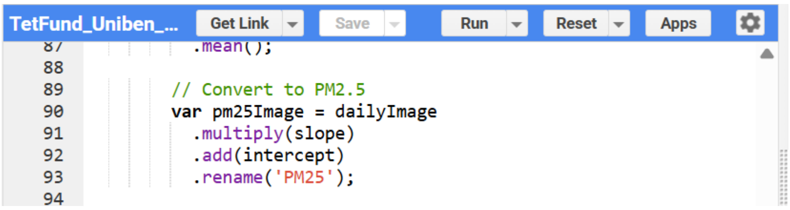

```javascript
        .mean();

      // Convert to PM2.5
      var pm25Image = dailyImage
        .multiply(slope)
        .add(intercept)
        .rename('PM25');

```

Figure 6: Regression Model Used to Estimate PM2.5 from AOD

Model Uncertainty and Validation

Due to the humid tropical characteristics of the study area, strict MAIAC quality assurance (QA) filtering was not fully enforced in order to preserve sufficient temporal coverage for long-term trend analysis. Previous studies have shown that aggressive QA filtering in tropical environments may remove a substantial proportion of valid observations due to persistent cloud contamination and atmospheric variability (Zhang *et al.*, 2017). Ground-based aerosol monitoring systems such as AERONET have significantly improved aerosol validation and calibration studies globally (Giles *et al.*, 2019; Holben *et al.*, 1998). To minimize uncertainty, only non-null observations were retained and monthly aggregation was applied to reduce short-term atmospheric noise.

The developed regression model was evaluated using the coefficient of determination (R²) and correlation coefficient (R). Additional residual assessment was conducted through visual inspection of regression dispersion patterns and comparison with an independent secondary monitoring location (Palm House Station). Although the calibration dataset was relatively limited ($n \approx 36$–50 valid observations depending on seasonal filtering), the analysis was intended primarily for seasonal aerosol characterization rather than high-precision PM₂.₅ exposure prediction.

Seasonal Analysis (Harmattan Period)

Due to data limitations during the wet season, analysis focused on the Harmattan period (November–March), when aerosol concentrations are highest.

To account for seasonal overlap across calendar years, a seasonal index was defined as shown in equation 10:

$$Season_{year} = Nov_t + Dec_t + Jan_{t+1} + Feb_{t+1} + Mar_{t+1} \quad (10)$$

Seasonal averages were computed as using equation 11:

$$\bar{X}_{season} = \frac{1}{n}\sum_{i=1}^{n} X_i \quad (11)$$

Trend Analysis

Trend analysis was carried out using two model's vis: Mann-Kendall and Sen's Slope Estimator:

Mann–Kendall Test

The Mann–Kendall test (Mann, 1945; Kendall, 1975) was used to detect monotonic trends. Equation 12 was particularly useful for achieving this task:

$$S = \sum_{i=1}^{n-1} \sum_{j=i+1}^{n} \operatorname{sign}(x_j - x_i) \quad (12)$$

Sen's Slope Estimator

Trend magnitude was estimated using Sen's slope (Sen, 1968) based on equation 13:

$$Q = median\left(\frac{x_j - x_i}{j - i}\right) \quad (13)$$

Statistical and Time-Series Analysis

All analyses were performed using Python libraries including:

i. Pandas which were used for (data handling)
ii. NumPy adopted for (numerical computation)
iii. Matplotlib, for (visualization)
iv. PyMannKendall used for (trend detection)

The analytical workflow is illustrated in Figure 7, showing the integration of satellite data processing and statistical modeling.

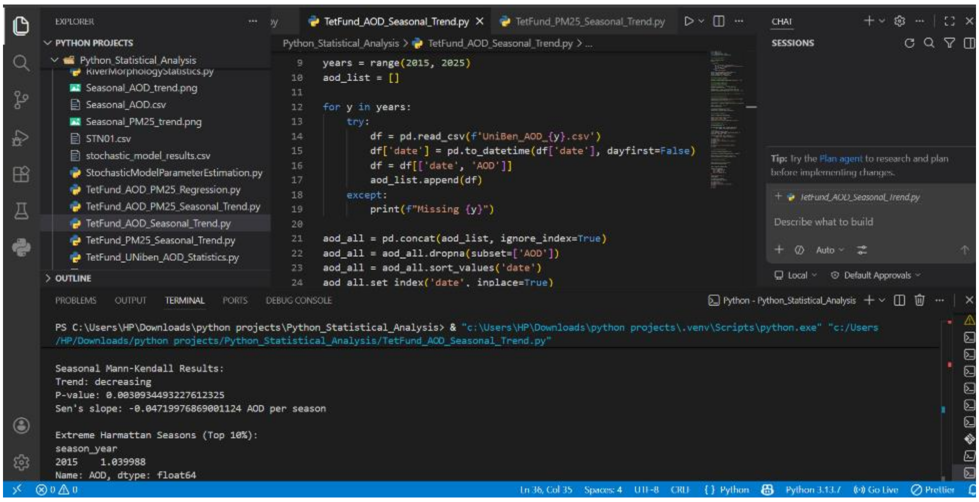

```python
years = range(2015, 2025)
aod_list = []

for y in years:
    try:
        df = pd.read_csv(f'UniBen_AOD_{y}.csv')
        df['date'] = pd.to_datetime(df['date'], dayfirst=False)
        df = df[['date', 'AOD']]
        aod_list.append(df)
    except:
        print(f"Missing {y}")

aod_all = pd.concat(aod_list, ignore_index=True)
aod_all = aod_all.dropna(subset=['AOD'])
aod_all = aod_all.sort_values('date')
aod_all.set_index('date', inplace=True)
```

```
PS C:\Users\HP\Downloads\python projects\Python_Statistical_Analysis> & "c:\Users\HP\Downloads\python projects\.venv\Scripts\python.exe" "c:/Users
/HP/Downloads/python projects/Python_Statistical_Analysis/TetFund_AOD_Seasonal_Trend.py"

Seasonal Mann-Kendall Results:
Trend: decreasing
P-value: 0.0030934493227612325
Sen's slope: -0.04719976869001124 AOD per season

Extreme Harmattan Seasons (Top 10%):
season_year
2015    1.039988
Name: AOD, dtype: float64
```

Figure 7: Python Workflow of Seasonal AOD on VsCode

Data Export and Integration

Processed AOD and PM₂.₅ datasets were exported from Google Earth Engine as CSV files and subsequently analyzed in Python. This approach ensured consistency and enhanced harmonization between remote sensing outputs and statistical analysis.

RESULTS AND DISCUSSION

Relationship Between AOD and PM$_{2.5}$

The statistical relationship between satellite-derived Aerosol Optical Depth (AOD) and ground-measured PM$_{2.5}$ concentrations was evaluated using linear regression based on monthly averaged observations spanning November 2020 to December 2024. The regression results indicate a moderate positive relationship, with a coefficient of determination $R^2 = 0.2916$ and correlation coefficient $R = 0.54$. This implies that approximately 29.2% of the variability in PM$_{2.5}$ concentrations can be associated with variations in atmospheric aerosol loading, while the remaining variability may be influenced by meteorological conditions, atmospheric mixing, humidity effects, and local emission variability. The regression plot illustrating this relationship is presented in Figure 8, where the linear trend demonstrates that increasing AOD values are associated with higher surface particulate concentrations.

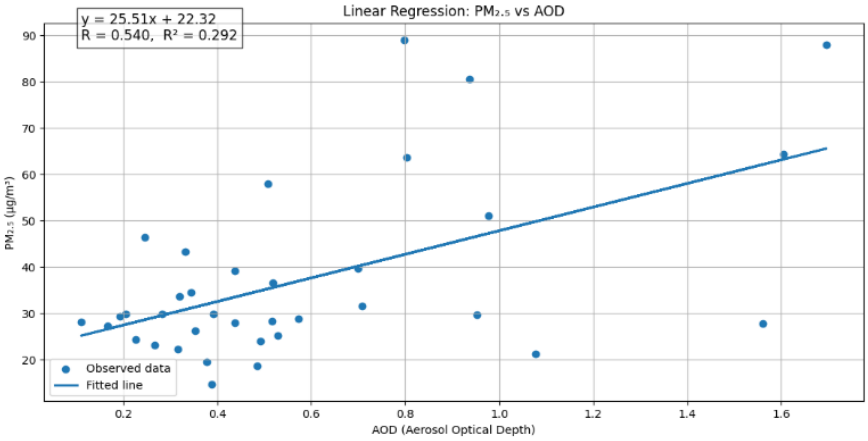

Figure 8: Linear Regression Plot

This finding is consistent with earlier studies by Gupta and Christopher (2009) and van Donkelaar et al. (2010), who demonstrated that AOD can provide useful proxy information for surface-level particulate matter, although the strength of the relationship is often reduced in humid tropical environments due to cloud cover, aerosol hygroscopic growth, and atmospheric instability. When the regression analysis was restricted to Harmattan months only, the coefficient of determination decreased to $R^2 = 0.23$, reflecting increased variability due to limited sample size and fluctuations in vertical aerosol distribution. Consequently, the all-months model was retained for subsequent $PM_{2.5}$ estimation because it provided relatively improved statistical stability and a larger calibration dataset compared to the Harmattan-only model. For validation, the Palm House dataset produced a stronger correlation ($R \approx 0.77$), indicating that aerosol–PM relationships tend to be stronger in highly urbanized environments with more consistent emission sources. However, the University of Benin model was retained to ensure spatial consistency with the study area.

Seasonal Data Availability

The availability of valid AOD observations during the Harmattan season (November–March) varied across the study period. The number of observations ranged from a minimum of 17 in 2015 to a maximum of 63 in 2016, with most years recording between 35 and 59 observations. This variability is primarily attributed to cloud contamination, aerosol retrieval uncertainty, and atmospheric interference, which commonly affect satellite observations in humid tropical regions. Nevertheless, the relatively higher data availability during the dry Harmattan season confirms that this period is optimal for aerosol analysis. The seasonal distribution of valid observations supports the methodological decision to focus on Harmattan months for trend analysis.

Seasonal Trend in Aerosol Optical Depth (AOD)

The Mann–Kendall test (equation 12) was applied to the seasonal AOD time series to evaluate long-term trends. The results indicate a statistically significant decreasing trend, with a p-value of 0.0031 ($p < 0.05$). The magnitude (Q) of the trend, estimated using Sen's slope (equation 13), was found to be: -0.046 AOD per season. This indicates a gradual reduction in atmospheric aerosol loading over the study period. Over the full duration (2015–2024), the cumulative decrease in AOD was approximately −0.519. The temporal evolution of seasonal AOD is presented in Figure 9, where the declining trend is clearly visible. The highest AOD value (~1.04) was observed during the 2015 Harmattan season, suggesting a period of intense aerosol concentration, likely associated with strong dust transport events.

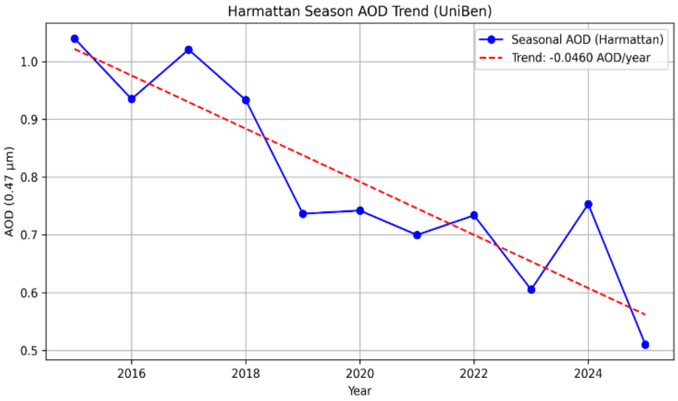

Figure 9: Seasonal AOD Trend

Although strict MAIAC quality assurance filtering was not fully implemented in this study, the use of monthly aggregation and exclusion of null observations helped reduce the influence of short-term atmospheric noise and preserve temporal continuity for long-term trend analysis. Similar decreasing trends in aerosol loading have been reported in other regional studies using satellite observations (Gavrouzou *et al*., 2021).

Seasonal Trend in $PM_{2.5}$ Concentration

Since $PM_{2.5}$ concentrations were derived from AOD using the regression model (equation 4), the trend analysis results are mathematically consistent with those of AOD. To assess robustness, two different calibration models were applied; all-months model (n = 50): $(PM_{2.5})$ the model is: $25.51 \cdot AOD + 22.32$ Harmattan-only model (n = 19); this model can be applied $PM_{2.5} = 21.13 \cdot AOD + c$. Both models yielded statistically significant decreasing trends (p = 0.0031), with Sen's slope values of approximately: −1.20 µg/m³ per season (all-months model) and −0.997 µg/m³ per season (Harmattan-only model). The consistency in trend direction across both calibration approaches suggests that the observed decline in $PM_{2.5}$ is relatively stable despite uncertainties associated with aerosol retrieval and model calibration. The temporal variation in $PM_{2.5}$ concentrations is illustrated in Figure 10.

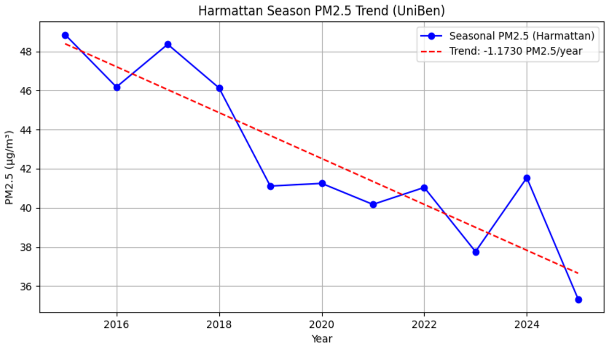

Figure 10: Seasonal PM2.5 Trend

Combined Interpretation of AOD and $PM_{2.5}$ Trends

A comparative analysis of AOD and $PM_{2.5}$ trends reveals strong agreement in both direction and magnitude. Both variables exhibit statistically significant decreasing trends, with similar temporal patterns and identical Mann–Kendall statistics. This agreement suggests that AOD can provide useful information for characterizing broad seasonal aerosol behaviour, although uncertainties associated with atmospheric humidity, boundary-layer dynamics, aerosol mixing, and satellite retrieval limitations remain important considerations. Furthermore, the consistency across different calibration approaches indicates that the observed decreasing trend is unlikely to be solely associated with methodological variability.

Descriptive Statistics

The descriptive statistics of seasonal AOD and $PM_{2.5}$ concentrations are presented in Table 1. AOD values exhibit moderate variability, with: Mean = 0.79; Minimum = 0.51; Maximum = 1.04 and Standard deviation = 0.17. Similarly, $PM_{2.5}$ concentrations show: Mean = 42.52 µg/m³; Range = 35.34–48.85 µg/m³ and Standard deviation = 4.32 µg/m³. The relatively close agreement between mean and median values indicates a stable distribution, while occasional higher values correspond to periods of intense aerosol loading during strong Harmattan events. This supports the suitability of the dataset for broad seasonal trend characterization despite inherent uncertainties associated with satellite-derived aerosol retrievals. The distributions of both variables are further illustrated in Figure 11 and Figure 12, which present histograms of seasonal $PM_{2.5}$ and AOD values, respectively.

Table 1: Descriptive Statistics of Seasonal AOD and $PM_{2.5}$

Variable	Mean	Minimum	Maximum	Std. Deviation
AOD	0.7918	0.5103	1.0400	0.1695
$PM_{2.5}$ (µg/m³)	42.52	35.34	48.85	4.32

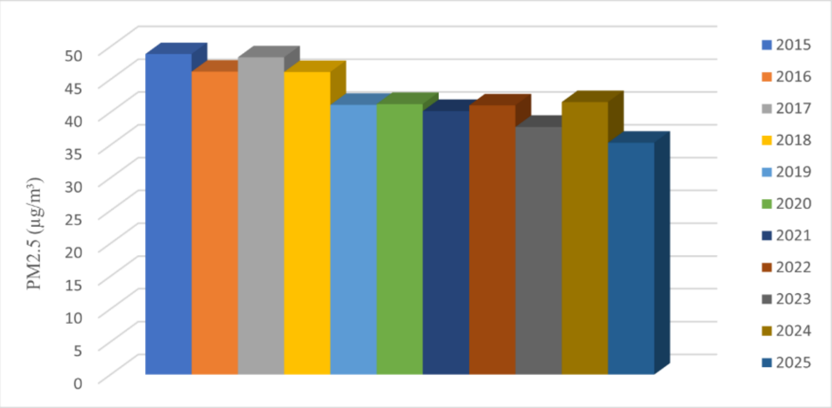

Figure 11: Histogram of Averaged Seasonal PM2.5

From Figure 11, the histogram reveals that $PM_{2.5}$ concentrations are moderately distributed within a relatively narrow range, indicating consistent seasonal aerosol conditions over the study period. The distribution appears approximately symmetric, with most values clustering around the mean (~42 µg/m³), suggesting a stable central tendency. The absence of extreme outliers indicates that although seasonal variations exist, there are no abnormal pollution spikes, and $PM_{2.5}$ levels remain within a predictable range during Harmattan periods. This supports the reliability of the dataset for long-term trend analysis.

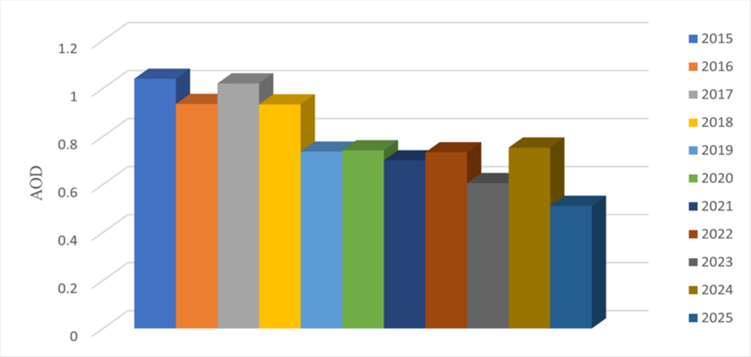

Figure 12: Histogram of Averaged Seasonal AOD

The histogram in Figure 12 shows that AOD values are moderately concentrated within the range of approximately 0.5 to 1.0, with a clear clustering around the mean (~0.79). This indicates consistent aerosol loading across seasons, with variations largely reflecting differences in dust transport intensity. The relatively smooth and unimodal distribution suggests that aerosol conditions are systematically influenced by seasonal processes, particularly Harmattan-driven dust influx, rather than random fluctuations.

Limitations

Despite the promising findings, several limitations must be acknowledged. First, the regression model explains only 29% of the variability in $PM_{2.5}$ concentrations. While this may appear low, it is consistent with similar studies conducted in tropical environments, where meteorological factors and atmospheric complexity weaken the AOD–PM relationship (Ma *et al*., 2019; Attey-Yeboah *et al*., 2025).

The absence of strict quality assurance (QA) filtering may introduce some uncertainty into the AOD dataset. However, studies have shown that applying strict QA filters in humid regions can result in the loss of more than 75% of observations (Zhang *et al*., 2017), making it impractical for long-term trend analysis. The $PM_{2.5}$ time series is derived from AOD, meaning that trend results are not entirely independent. While ground-based data were used for calibration, they do not cover the full temporal range of the study.

Another important limitation relates to the temporal mismatch between satellite overpass observations and ground-based $PM_{2.5}$ measurements. MODIS observations represent near-instantaneous atmospheric conditions during satellite overpass periods, whereas the ground-based measurements were aggregated into broader temporal intervals. In addition, the use of spatial averaging across the entire study area rather than station-buffer collocation may reduce sensitivity to localized aerosol variability. Atmospheric humidity, boundary-layer height, and aerosol vertical distribution may also influence the observed AOD–$PM_{2.5}$ relationship.

The regression model does not incorporate meteorological variables such as humidity, boundary layer height, and wind speed, which are known to influence aerosol behaviour (Gupta & Christopher, 2009; van Donkelaar *et al*., 2010). Finally, the model is spatially limited to the University of Benin environment and may not be directly transferable to other regions without recalibration.

CONCLUSION

This study developed a satellite-based framework for estimating and analyzing $PM_{2.5}$ concentrations over the University of Benin using MODIS MAIAC Aerosol Optical Depth (AOD) data integrated with ground-based observations. The results revealed a moderate positive relationship between AOD and $PM_{2.5}$ concentrations, with a correlation coefficient of 0.54 and coefficient of determination (R^2) of 0.29. Although the explanatory strength of the regression model is moderate, the observed relationship remains meaningful for tropical environments where atmospheric humidity, cloud contamination, aerosol mixing, and boundary-layer variability commonly weaken the AOD–$PM_{2.5}$ linkage.

Seasonal Mann–Kendall trend analysis revealed a statistically significant decreasing trend in Harmattan aerosol loading over the study period (2015–2024), with a Sen's slope of approximately −0.046 AOD per season. Similarly, the estimated $PM_{2.5}$ concentrations showed decreasing seasonal trends ranging from approximately −0.997 to −1.20 µg/m³ per season across different calibration approaches. The consistency in trend direction suggests that the observed decline reflects a relatively stable environmental signal despite uncertainties associated with satellite retrievals and model calibration.

The study further demonstrated that satellite-derived aerosol observations, when locally calibrated with available ground measurements, can provide useful insight into seasonal aerosol behaviour and long-term environmental trends in data-limited tropical environments. While the developed regression framework is more suitable for seasonal characterization than high-precision $PM_{2.5}$ prediction, the approach offers practical value for campus-scale environmental monitoring, low-cost air-quality surveillance, and preliminary public-health exposure assessment. Future studies should integrate meteorological variables, quality-assured aerosol retrievals, and machine learning approaches to further improve $PM_{2.5}$ estimation accuracy and environmental interpretation.

ACKNOWLEDGMENT

The authors are very grateful to the sponsor. This research was funded by the TETFUND-IBR 2024/2025 Batch 20 (19).

REFERENCES

Attey-Yeboah, P., Afful, C., Yeboah, K., Korkpoe, C. H., Coker, E. S., Subramanian, R., & Amegah, A. K. (2025). Utility of low-cost sensor measurement for predicting ambient $PM_{2.5}$ concentrations: Evidence from a monitoring network in Accra, Ghana. *Environmental Science: Atmospheres, 5*, 517–529. https://doi.org/10.1039/D4EA00140K

Bodhaine, B. A., Wood, N. B., Dutton, E. G., & Slusser, J. R. (1999). On Rayleigh optical depth calculations. *Journal of Atmospheric and Oceanic Technology, 16*(11), 1854–1861.

Chauhan, B. V. S., Verma, S., Rahman, B. M. A., & Wyche, K. P. (2025). Deep learning in airborne particulate matter sensing and surface plasmon resonance for environmental monitoring. *Atmosphere, 16*(4), 359. https://doi.org/10.3390/atmos16040359

Chew, B. N., Campbell, J. R., Hyer, E. J., Salinas, S. V., Reid, J. S., Welton, E. J., Holben, B. N., & Liew, S. C. (2016). Relationship between aerosol optical depth and particulate matter over Singapore. *Aerosol and Air Quality Research, 16*(11), 2818–2830. https://doi.org/10.4209/aaqr.2015.07.0457

Chylek, P., Henderson, B. G., & Lesins, G. (2005). Aerosol optical depth retrieval over NASA Stennis Space Center. *IEEE Transactions on Geoscience and Remote Sensing, 43*(9), 1978–1983.

Draper, N. R., & Smith, H. (1998). *Applied regression analysis* (3rd ed.). John Wiley & Sons.

Eckhardt, C. M., & Wu, H. (2021). Environmental exposures and lung aging. *Current Environmental Health Reports, 8*(4), 281–293.

Gavrouzou, M., Hatzianastassiou, N., Gkikas, A., Korras-Carraca, M.-B., & Mihalopoulos, N. (2021). Global climatology of dust aerosols. *Remote Sensing, 13*(3), 359.

Giles, D. M., et al. (2019). AERONET Version 3 database. *Atmospheric Measurement Techniques, 12*, 169–209.

Gupta, P., & Christopher, S. A. (2009). PM estimation using satellite and meteorological data. *Journal of Geophysical Research: Atmospheres, 114*.

Holben, B. N., et al. (1998). AERONET aerosol monitoring network. *Remote Sensing of Environment, 66*(1), 1–16.

Hu, Z., & Rao, K. R. (2009). Air pollution and heart disease. *Environmental Health, 8*, 26.

Kasten, F., & Young, A. T. (1989). Optical air mass tables. *Applied Optics, 28*(22), 4735–4738.

Kendall, M. G. (1975). *Rank correlation methods* (4th ed.). Charles Griffin.

Li, T., Wang, Y., & Wu, J. (2024). Satellite $PM_{2.5}$ estimation using ML. *npj Climate and Atmospheric Science, 7*, 138.

Logothetis, S.-A., et al. (2024). Machine learning AOD retrieval. *Remote Sensing, 16*(7), 1132.

Lyapustin, A., Wang, Y., Korkin, S., & Huang, D. (2018). MODIS MAIAC algorithm. *Atmospheric Measurement Techniques, 11*, 5741–5765.

Ma, Y., Xin, J., Zhang, W., Liu, Z., Ma, Y., Kong, L., Wang, Y., Deng, Y., Lin, S., & He, Z. (2019). Long-term variations of the PM2.5 concentration identified by MODIS in the tropical rain forest, Southeast Asia. *Atmospheric Research, 219*, 140–152. Doi: https://doi.org/10.1016/j.atmosres.2018.12.024

Mann, H. B. (1945). Non-parametric test against trend. *Econometrica, 13*(3), 245–259. Doi: https://doi.org/10.2307/1907187

Montgomery, D. C., Peck, E. A., & Vining, G. G. (2012). *Introduction to linear regression analysis* (5th ed.).

National Aeronautics and Space Administration (NASA., 2026). MODIS missions and measurements. Retrieved May 15, 2025. From https://www.earthdata.nasa.gov/data/instruments/modis

Ogunjo, S., Olaniyan, O., Olusegun, C. F., Kayode, F., Okoh, D., & Jenkins, G. (2022). The role of meteorological variables and aerosols in the transmission of COVID-19 during harmattan season. GeoHealth, 6, e2021GH000521. Doi: https://doi.org/10.1029/2021GH000521

Pham-Duc, B., Nguyen, H., Phan, H., & Tran-Anh. (2023). Trends and applications of Google Earth Engine in remote sensing and earth science research: A bibliometric analysis using Scopus database. *Earth Science Informatics, 16*, 2355–2371. Doi: https://doi.org/10.1007/s12145-023-01035-2

Rahal, F. (2020). Low-cost air quality sensors. *Clean Air Journal, 30*(2), 1–2.

Ramírez, O., Hernández-Cuellar, B., & de la Rosa, J. D. (2023). Air quality monitoring on university campuses as a crucial component to move toward sustainable campuses: An overview. *Urban Climate, 52*, 101694. Doi: https://doi.org/10.1016/j.uclim.2023.101694

Sen, P. K. (1968). Estimates of the regression coefficient based on Kendall's tau. *Journal of the American Statistical Association, 63*(324), 1379–1389. Doi: https://doi.org/10.1080/01621459.1968.10480934

United Nations Environment Programme. (2021). *Global environment outlook for cities*.

van Donkelaar, A., Martin, R. V., Brauer, M., Kahn, R., Levy, R., Verduzco, C., & Villeneuve, P. J. (2010). Global estimates of ambient fine particulate matter concentrations from satellite-based aerosol optical depth: Development and application. *Environmental Health Perspectives, 118*(6), 847–855. https://doi.org/10.1289/ehp.0901623

Zhang, M., Huang, B., & He, Q. (2017). An evaluation of four MODIS Collection 6 aerosol products in a humid subtropical region. *Remote Sensing, 9*(11), 1173. https://doi.org/10.3390/rs9111173